

# Visible-Light Driven Oxidation of Water as Catalyzed by Co-APO-5 in the Presence of Ru Sensitizer

Marco Armandi,<sup>†,‡</sup> Simelys Hernandez,<sup>†</sup> Svetoslava Vankova,<sup>‡</sup> Simone Zanarini,<sup>‡</sup> Barbara Bonelli,<sup>‡</sup> and Edoardo Garrone<sup>\*‡</sup>

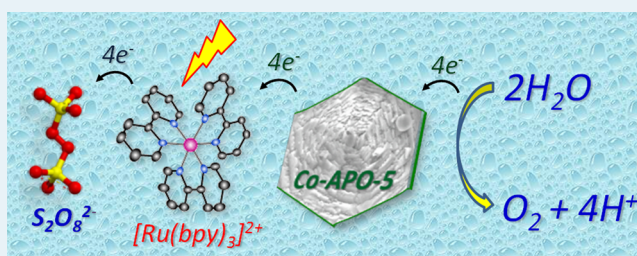
<sup>†</sup>Center for Space Human Robotics IIT@Polito, Istituto Italiano di Tecnologia, Corso Trento 21, 10129 Torino, Italy

<sup>‡</sup>Dipartimento di Scienza Applicata e Tecnologia and INSTM Unit Torino-Politecnico, Politecnico di Torino, Corso Duca degli Abruzzi 24, 10129 Torino, Italy

## S Supporting Information

**ABSTRACT:** Cobalt aluminum phosphate with AFI zeolitic structure (Co-APO-5) catalyzes light-driven water oxidation (WO) when both the ruthenium complex  $[\text{Ru}(\text{bpy})_3]^{2+}$ , as photosensitizer, and persulfate species  $\text{S}_2\text{O}_8^{2-}$ , as sacrificial electron acceptor, are present. Measurements have been run in a flow reactor, allowing the amount of oxygen evolved to be evaluated and, in particular, the initial rate of WO reaction to be measured. The latter has been studied as a function of chemical composition, and some kinetic features have been established. Competitive reactions occur extensively, causing the oxidation of the Ru complex to the detriment of oxygen production. The initial rate of WO increases with the amount of catalyst until turbidity of the suspension sets in. A reaction order close to  $-1$  with respect to persulfate was found, which indicates the occurrence of surface processes involving Co centers at the outer layer of Co-APO-5 particles (accessed by the bulky  $[\text{Ru}(\text{bpy})_3]^{2+}$  species, at variance with Co species in the core), for the adsorption onto which competition takes place between the Ru complex and persulfate species. A less pronounced negative order (ca.  $-0.4$ ) for the sensitizer was also observed, for which an interpretation is proposed.

**KEYWORDS:** water oxidation catalyst, Co-APO-5,  $[\text{Ru}(\text{bpy})_3]^{2+}$ , chemical reactor



## INTRODUCTION

Photochemical water splitting (WS) to molecular hydrogen and oxygen is an attractive strategy for storing the abundant solar energy impinging on Earth into chemical bonds.<sup>1</sup> Between the two involved half-reactions, water oxidation (WO) to molecular oxygen is the more challenging and usually considered as the bottleneck of the whole WS process, because it involves multiple proton-coupled electron transfer processes. Therefore, the development of an effective WO catalyst is the focus of intense research.

In this broad context, already in the 1980s studies were reported on the catalytic activity of aqueous cobalt(II) ions<sup>2–4</sup> and cobalt oxide.<sup>5</sup> More recently, the interest in Co ions as active ingredients in the catalysts for light-driven WS has grown, as reviewed by Fontecave and co-workers.<sup>6</sup> For instance, Frei and co-workers<sup>7</sup> have shown that  $\text{Co}_3\text{O}_4$  dispersed in SBA-15 silica catalyzes the photoassisted WO reaction, when the  $[\text{Ru}(\text{bpy})_3]^{2+}$  complex acts as a sensitizer and the produced electrons are scavenged by sodium persulfate  $\text{Na}_2\text{S}_2\text{O}_8$ . Graetzel<sup>8</sup> in a different approach has proposed the use of hematite as a semiconductor where absorption of light can form electron/hole pairs then reacting with water: doping of hematite with Co ions has been, however, shown to be beneficial. Nocera and co-workers have reported<sup>9</sup> that a system

of ITO/Co ions in a phosphate solution splits water with a remarkably reduced electrical bias, because a surface phase is formed implying clusters of Co ions. More recently, Nocera and associates have proposed a device where the electron/hole separation occurs in a Si wafer, employing the same Co catalyst at the anode side.<sup>10</sup> Other very recent papers deal with the role in water splitting of Co(II) adsorbed onto silica nanoparticles,<sup>11</sup> of Co oxide on graphene,<sup>12</sup> and of Co cations on the efficiency of  $\text{WO}_3$  and  $\text{BiVO}_4$  photoanodes.<sup>13,14</sup>

Besides Co-containing solid phases, several Co-based molecular species were found to act as homogeneous catalysts for WO.<sup>15–19</sup> In many cases, the active center is a cobalt-oxo cubical structure resembling the catalytic core universally found in photosynthetic enzymes that catalyze water oxidation and also proposed for Nocera's catalyst.

On the spur of the growing interest for the role of Co cations in WS, we have undertaken a study of the reactivity toward liquid water of Co ions embedded in porous aluminum phosphates (APO systems), the goal being the control of their coordination and valence state through the crystalline structure

Received: April 19, 2012

Revised: March 25, 2013

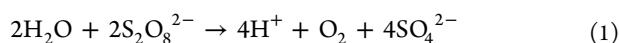
Published: April 4, 2013

of the matrix. Studies concerning other solid Co-containing systems will follow.

In APO systems (e.g., the one showing the AFI zeolitic structure, APO-5), several divalent or trivalent cations can substitute for Al (giving rise to Me-APO systems), in particular both  $\text{Co}^{2+}$  and  $\text{Co}^{3+}$ . With divalent cations, a charge-balancing chemical object (e.g., a proton) is present.<sup>20</sup> Me-APO systems are well-known in catalysis, and their “dry” chemistry (in particular that of Co-APO) has been studied in detail.<sup>21,22</sup>

In contrast, the aqueous chemistry of such systems, and in particular their behavior in the WS reaction, has never been examined. We have found that Co-APO-5 samples activated in an oxidizing medium, featuring ca. 15% of Co in the trivalent state, react with liquid water at room temperature with evolution of oxygen,<sup>23</sup> because of the instability in an aqueous system of  $\text{Co}^{3+}$  cations in octahedral coordination,<sup>24</sup> which turn into divalent Co ions.

On the other hand, we have recently reported that Co-APO-5 samples featuring  $\text{Co}^{2+}$  are able to photochemically split water if an electric bias is applied.<sup>25</sup> We report now on the ability of the same  $\text{Co}^{2+}$  cations embedded in the APO structure to promote the WO reaction when both a sacrificial reactant (Sodium persulfate) and a sensitizer (the  $\text{Ru}(\text{bpy})_3\text{Cl}_2$  complex) are present. The stoichiometry is



The commonly accepted mechanism will be described below. Note that a buffer is required due to the extensive formation of hydronium ions.

In the present work, an open reactor operating under Ar flow has been adopted, so to have a standard way of measuring the rate of oxygen evolution (OE) and thus to establish some kinetic features of the WO process.

## EXPERIMENTAL SECTION

**Material.** Co-APO-5 material was synthesized according to ref 26. Standard Al and P sources were used in a sol–gel procedure, *N,N*-diethyl-ethanolamine (DEA) was used as template, and cobalt acetate was added to the gel phase, to reach the nominal composition  $0.9\text{Al}_2\text{O}_3/1.0\text{P}_2\text{O}_5/0.1\text{CoO}/1.6\text{DEA}/80\text{H}_2\text{O}$ . The gel was crystallized in a Teflon-lined autoclave at 473 K for 3 days; the organic template was then removed by calcination under flowing oxygen at 823 K.

Cobalt content in the fresh catalyst is ca. 3.0 wt %, as determined by ICP-AES (Perkin-Elmer OPTIMA 7000 DV ICP/OES). The quality of prepared Co-APO-5 material was checked by means of several techniques, including  $\text{N}_2$  adsorption/desorption at 77 K, XRD, FE-SEM, and UV–vis spectroscopy. Because this part of the work is not original (the obtained material is fully comparable with those described in the literature), related results are reported only as Supporting Information.

An estimate of Co ions on the external surface of Co-APO-5 (thought to be active, *vide infra*) was carried out from the total metal content (3 wt %) and the ratio between external and total surface area (Supporting Information, p 1): the corresponding amount is  $3.4 \mu\text{mol}$  in 100 mg of the catalyst.

Moreover, because the fraction of Co ions able to change valence state is ca. 15% of the total,<sup>22</sup> the amount of active Co in the sample is reckoned to be  $0.51 \mu\text{mol}$ . After reaction, the catalyst was analyzed by ICP-atomic emission spectrometry, and a total Co content of ca. 2.5% was observed because of some leaching.

**Experimental Set Up.** Figure 1 illustrates the reactor used, consisting of a quartz cylinder with total volume 190 mL containing 100 mL of solution, into which Ar flows (at a rate ( $Q_{\text{Ar}}$ ) of 5 N·mL/min) by bubbling into the liquid phase, kept homogeneous through a magnetic stirrer (950 rpm). The reactor has a glass window allowing illumination with visible light obtained by filtering the radiation from a

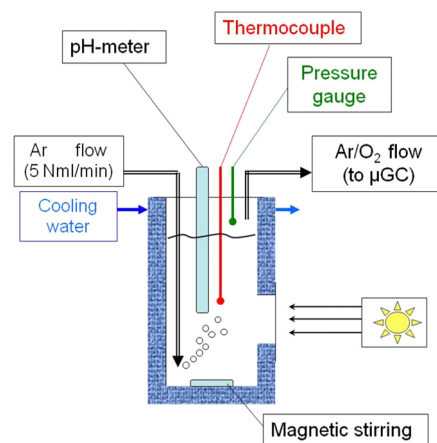


Figure 1. Scheme of the flow reactor.

450 W xenon arc lamp through a Newport filter (model FSQ-KQ2). The lamp was positioned to have an incident power of  $50 \text{ mW}/\text{cm}^2$ , as measured using a power meter (Delta OHM HD 2102.1).

Inside the reactor, total pressure ( $P$ ) is slightly higher than the outside atmosphere (1.06 atm) and temperature ( $T$ ) is maintained at  $T = 20 \text{ }^\circ\text{C}$  through the use of an external jacket with cooling water. The oxygen concentration ( $C_{\text{O}_2}$  [ppm]) in the outgoing mixture is measured every minute through a micro-gas chromatograph (Varian 490- $\mu\text{GC}$ ) equipped with a capillary column Molsieve 5A (10 m length) and a micro-TCD detector. The actual oxygen flow  $\Phi(\text{O}_2)$  [ $\mu\text{mol min}^{-1}$ ] is given by 2:

$$\Phi(\text{O}_2) = \frac{\left(\frac{C_{\text{O}_2}}{1 - C_{\text{O}_2}}\right)PQ_{\text{Ar}}}{RT} \quad (2)$$

where  $R$  is the ideal gas constant [ $0.082 \text{ L atm mol}^{-1} \text{ K}^{-1}$ ]. Integration of  $\Phi(\text{O}_2)$  over time elapsed yields the total amount of evolved  $\text{O}_2$ .

**Procedure for Kinetic Measurements.** The oxygen flow  $\Phi(\text{O}_2) = \Phi(\text{O}_2)(t)$  as detected by the gas chromatograph does not represent the oxygen production rate in solution  $dn_{\text{O}_2}/dt = (dn_{\text{O}_2}/dt)(t)$ , which is the really relevant observable. A way, however, to evaluate this latter is as follows.

A constant rate of oxygen production can be mimicked by a mock reaction, actually a sweeping experiment, where first pure Ar is bubbled through the solution until  $\text{O}_2$  and  $\text{N}_2$  are no longer detected, then a constant concentration of oxygen is added ( $C_{\text{O}_2}^*$ ), keeping the gas flow ( $Q$ ) constant to  $5 \text{ N}\cdot\text{mL min}^{-1}$ . The input of moles of oxygen per unit time,  $dn_{\text{O}_2}/dt$  equals  $\Phi_{\text{O}_2}^*$ . Figure 2a reports the curves obtained for five different values of the oxygen flow ( $\Phi_{\text{O}_2}^*$ ). All curves just differ by a scale factor, and have all an exponential trend, the plateau value corresponding to the adopted oxygen concentration being reached after ca. 40 min. The initial portion of the curves is linear, the corresponding slopes  $[d\Phi_{\text{O}_2}/dt]_0$  being proportional to the plateau values  $\Phi_{\text{O}_2}^*$  (Figure 2b). The interpretation of the whole of Figure 2 is straightforward: results are simply due to the stripping of the gaseous section of the reactor (headspace dead volume,  $V_g$ ) according to mass balance in eq 3:

$$QC_{\text{O}_2}^* = QC_{\text{O}_2} + V_g dC_{\text{O}_2}/dt \quad (3)$$

which gives

$$C_{\text{O}_2} = C_{\text{O}_2}^*[1 - \exp(-tQ/V_g)] \quad (4)$$

or through eq 2

$$\Phi_{\text{O}_2} = \Phi_{\text{O}_2}^*[1 - \exp(-tQ/V_g)] \quad (5)$$

from which

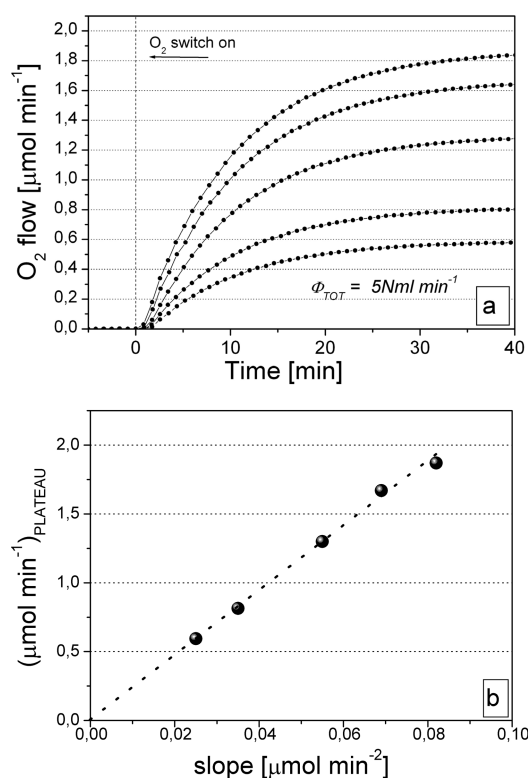


**Figure 2.** Injection of a constant oxygen concentration ( $C_{O_2}^*$ ) into the Ar flow (mock reaction): (a) oxygen flow curves as measured by  $\mu$ -GC; (b) correlation plot between initial slopes  $[d\Phi_{O_2}/dt]_0$  and  $\Phi_{O_2}^*$ .

$$[d\Phi_{O_2}/dt]_0 = \Phi_{O_2}^*(V_g/\Phi) \quad (6)$$

The meaning of eq 6 is that the slope  $[d\Phi_{O_2}/dt]_0$  can be assumed as a measure of the initial rate of reaction  $[dn_{O_2}/dt]_0$ . The validity of this result has been further checked in a separate set of experiments, implying the direct measurement of oxygen formed in solution (through a Clark electrode). For this, a catalytic system already known to be active in WO<sup>7</sup> was used. Because this part of the work is only preliminary to the results of the actual investigations, related data are reported only in Supporting Information (Figures S5 and S6).

**Types of Experiments.** The reaction mixture had, as constant parameters, 100 mL of buffer (60 mM NaHCO<sub>3</sub> + Na<sub>2</sub>SiF<sub>6</sub>, with starting pH = 6.0, and 390 mg of Na<sub>2</sub>SO<sub>4</sub>, corresponding to a 27 mM concentration). Prior to each measurement, Ar was flowed through the reactor until traces of O<sub>2</sub> and N<sub>2</sub> were no longer detected. Note that the chemical composition adopted follows the recipe used in ref 7. Future work will elucidate whether such conditions are those optimal for the present case.

Three types of measurements were carried out: (1) the amount of Na<sub>2</sub>S<sub>2</sub>O<sub>8</sub> was maintained at 260 mg (corresponding to a 11 mM solution) and that of Ru(bpy)<sub>3</sub>Cl<sub>2</sub> at 45 mg (0.6 mM), whereas the amount of the Co-APO-5 catalyst in aqueous suspension was 100, 250, 500, or 800 mg; (2) the amount of Co-APO-5 and Ru(bpy)<sub>3</sub>Cl<sub>2</sub> was 250 mg and 45 mg (0.60 mM), respectively, and that of persulfate was varied at 65, 260, and 500 mg (3, 11, and 21 mM, respectively); in these cases, at the end of each measurement, the same amount of persulfate was added, and a second run was performed; (3) two measurements were run with different dye content (70, 45, and 20 mg, corresponding to 0.93, 0.60, and 0.27 mM, respectively), while the amounts of Co-APO-5 and persulfate were 250 and 260 mg, respectively. The pH did not vary significantly through all the measurements, being in the 6.0–5.7 range, because of the buffer.

Blank experiments were carried out, which showed that no oxygen was released in the absence of one of the ingredients. Moreover, no oxygen evolution was observed when Co ions were present in solution

as cobalt acetate in place of Co-APO-5 ( $[Co^{2+}] = 50 \mu M$ ;  $[Ru(bpy)_3^{2+}] = 0.6 \text{ mM}$ ;  $[S_2O_8^{2-}] = 11 \text{ mM}$ ). This is well noteworthy, because it means that none of the following results can be ascribed to leached Co species. Also, it must be stressed that Co<sup>2+</sup> species in solution may be active in WO, as documented already several years ago.<sup>2–4</sup> However, no activity was found with the present chemical composition: it is probable that the composition of the reacting system (e.g., buffering species) inhibits a possible role of Co<sup>2+</sup> ions otherwise active.

In a separate experiment, after a run with 250 mg of catalyst, 45 mg of Ru complex, and 65 mg persulfate, the catalyst was separated from the supernatant, rinsed in pure water, and used again in a new experiment with the same amounts of reactant. The results obtained in the second run were basically the same as in the first run.

## RESULTS AND DISCUSSION

Results reported in all the following figures show that Co-APO-5 systems are active in the WO reaction, as expected on the basis of the photoelectrochemical results.<sup>25</sup> Consider, for example, Figure 3a, which reports the set of data obtained

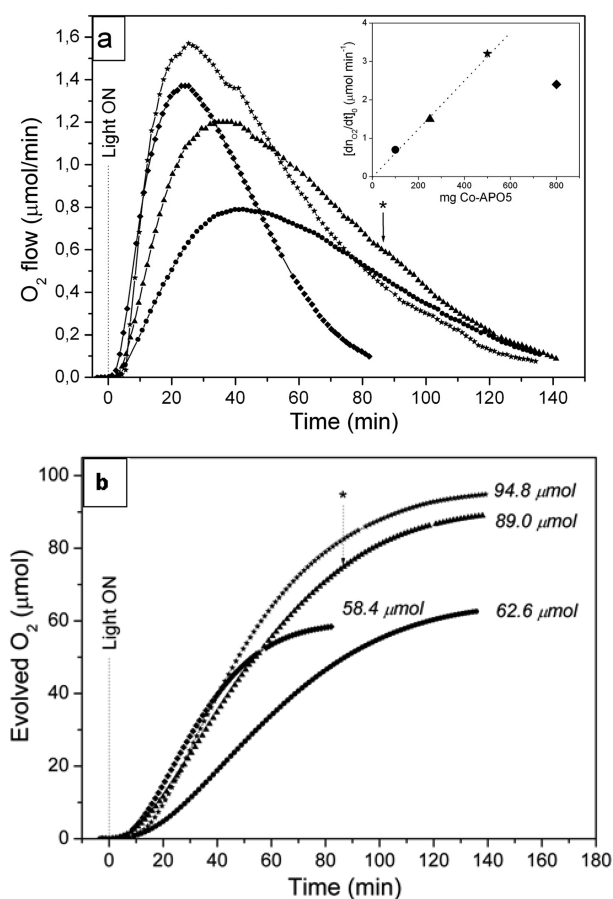


**Figure 3.** (a) Oxygen evolution curves with different amounts of Co-APO-5 catalyst: (●) 100 mg; (▲) 250 mg; (★) 500 mg; (◆) 800 mg. The arrow indicates lamp shutdown. Inset shows the initial rate of reaction  $[dn_{O_2}/dt]_0$ , as a function of the amount of catalyst. (b) Corresponding integral amounts of evolved oxygen.

when the amount of the Co-APO-5 catalyst was varied. Typically, after switching on the lamp, an induction period is observed of ca. 6 min (already observed with mock experiments but limited to 2–3 min) with negligible oxygen flow; then an almost linear portion follows, after which a peak is observed and a steady nearly exponential decline. The reason for a more



marked induction period is most probably that slow diffusion processes take place at the solid/gas interface, besides those at the liquid/gas interface.

The linear portion is expected, on the basis of the results in Figure 2, for a constant rate of reaction: this extends over a period of time large enough to allow a reasonably good value of the rate of the WO reaction, used, for example, in the inset to Figure 3.

The possible reasons for the decline in oxygen flow are several. The most straightforward is the depletion of the persulfate reactant. Indeed, if the lamp is switched off (Figure 3, arrow) when the oxygen flow is declining, no discontinuity in the curve is observed: we take this as evidence that the production of oxygen at this point is negligible, and mere stripping of the oxygen in the headspace and the dissolved oxygen in the liquid phase takes place. Indeed, the addition of persulfate to a postreacted system (empty symbols in Figure 4)

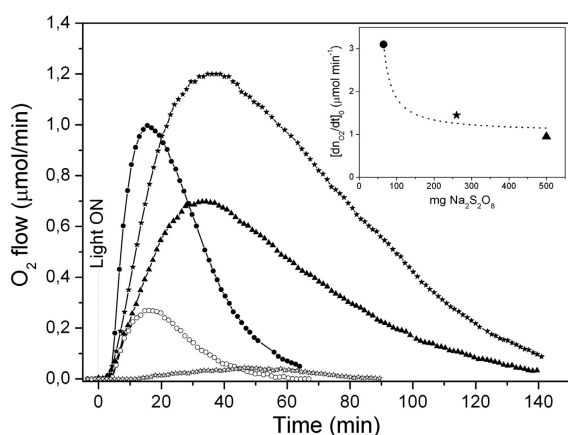
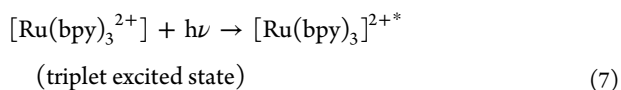


**Figure 4.** Oxygen evolution curves with different amounts of persulfate: (●) 65 mg; (★) 260 mg; (▲) 500 mg; second run experiment (empty symbols) performed after adding another 65 mg of persulfate. Inset shows initial rate of reaction  $[dn_{O_2}/dt]_0$  (of the first run), as a function of the amount of persulfate.

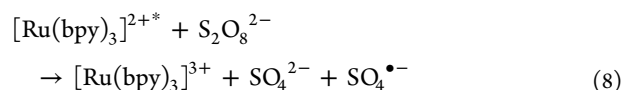
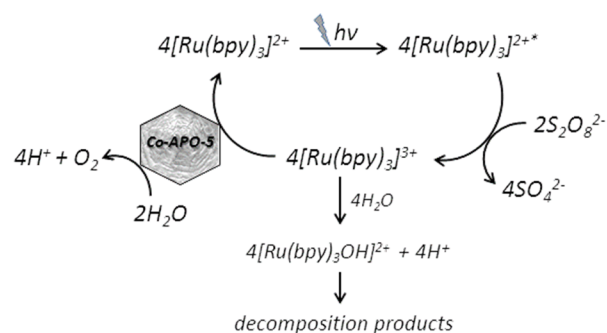
shows that the activity in oxygen production starts again: this is, however, definitely smaller than what is observed in the first run. This is evidence that depletion of persulfate is not the only cause for the decline in oxygen production:  $[\text{Ru}(\text{bpy})_3]^{2+}$  degradation has occurred quite substantially, as also suggested by comparison of UV-vis spectra of the reaction solution before and after water oxidation experiment (Figure S7, Supporting Information).

Further evidence on this point comes from the plots in Figure 3b, concerning integral amounts: the final values are much smaller than what is expected on the basis of stoichiometry (1 mol of  $O_2/2$  mol of  $S_2O_8^{2-}$ ) and correspond only to yields ( $Y$ ) of 11.5%, 16.3%, 17.4%, and 10.7% with respect to persulfate amounts when 100, 250, 500, and 800 mg of catalyst are used, respectively. More than 80% of the oxidizing capacity of persulfate concerns the Ru complex and not water.

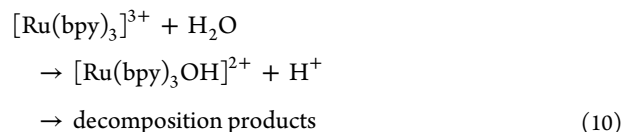
Let us consider the commonly accepted scheme (Scheme 1) for photoinduced WO sensitized by the Ru complex and assisted by persulfate as sacrificial acceptor:<sup>27–30</sup>



### Scheme 1. Schematic Representation of the Pathways Leading to Water Oxidation or to Depletion of Sensitizer

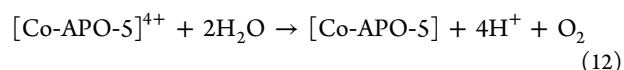
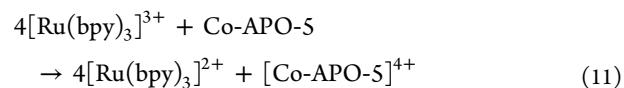


Step 7 is the excitation of the  $\text{Ru}^{2+}$  complex caused by absorption of light. The oxidized form of the sensitizer  $[\text{Ru}(\text{bpy})_3]^{3+}$  arises from both (i) an oxidative quenching reaction between  $S_2O_8^{2-}$  and the excited dye  $[\text{Ru}(\text{bpy})_3]^{2+*}$  (step 8) and (ii) a reaction between  $[\text{Ru}(\text{bpy})_3]^{2+}$  and the radical  $SO_4^{\bullet-}$  produced (step 9). Note that two photons and the consumption of two  $S_2O_8^{2-}$  generate four  $[\text{Ru}(\text{bpy})_3]^{3+}$ . Two fates are possible for the  $\text{Ru}^{3+}$  complex: either it is reduced back to the divalent state by the catalyst, as detailed below, with eventual yield of oxygen, or it undergoes a nucleophilic attack by water or hydroxide anions on bipyridine rings<sup>3,29</sup> of the type



The relative extent of the two processes (oxygen formation or oxidative degradation of the sensitizer) is a function of the relative rates: in the present case, the step yielding  $O_2$  seems to be definitely slower than that of the competitive reaction.

As to the WO reaction, making reference to established mechanisms (e.g., for colloidal iridium oxide), one may write a redox reaction involving the catalyst (step 11), followed by the oxidation of water (step 12) with release of protons:



On purpose, the generic expression  $[\text{Co-APO-5}]^{4+}$  is used in eqs 11 and 12, just to indicate that the accumulation of four holes at the catalytic site, whatever its nature, is required for water oxidation to oxygen and  $[\text{Ru}(\text{bpy})_3]^{2+}$  regeneration.

Actually, two meanings seem possible for the expression  $[\text{Co-APO-5}]^{4+}$ . The redox catalytic behavior of Co-APO-5 is generally accounted for invoking the chemistry of isolated framework Co(II)/Co(III) sites,<sup>20</sup> in that  $\text{Co}^{2+}$  ions (incorporated in tetrahedral framework positions forming  $\text{Co}(\text{OH})\text{P}$  Brønsted groups) can be involved in reversible Co(II)/Co(III) redox cycles.<sup>31,32</sup> The species  $[\text{Co-APO-5}]^{4+}$  could thus

correspond to four independent redox events involving four Co centers. These may be conceived as independent. We note, however, that Co ions in framework positions in Co-APO-5 are known to form Co–O–P–O–Co clusters with five or six neighboring Co atoms,<sup>33</sup> so that WO activity of Co-APO-5 could be related to such clusters, where Co ions may alternate between the divalent and trivalent states. Alternatively, one may invoke the formation of species Co(IV) as suggested by early studies<sup>2,3</sup> on WO reaction catalyzed by Co<sup>2+</sup> ions in solution in the presence of [Ru(bpy)<sup>3+</sup>], as well as by recent works<sup>34</sup> on Co-Pi WO catalyst. Note that such high-valence chemistry is in agreement with what is known about natural enzymes for WS, notably PSII. The question of the actual mechanism is outside the scope of this work.

The presence of competitive reactions makes it necessary to study the rate of oxygen evolution in the early stages of reaction, where decomposition of the Ru complex should be less extensive and the concentration of persulfate reasonably constant. This is exactly the region where linear growth of the oxygen partial pressure is observed.

As a matter of fact, in the series of measurements reported in Figure 3 where the amount of catalyst was varied, the rate is found to be proportional to the amount of catalyst (inset to Figure 3a), as expected. Only for the most loaded system a deviation is observed. A reason for such deviation is the increase in turbidity of the liquid phase because of the large mass of solid present. Similar effects of catalyst concentration on O<sub>2</sub> production rate have been observed for IrO<sub>2</sub>-based<sup>35</sup> WO catalysts. The explanation, there, is a competition occurring between step 9 above and the release of an electron to a catalytic site, instead of a persulfate. We are inclined to discard such explanation in the present case, because, whereas the oxidation state 3+ is acceptable for Ir, that of +1 is much less so for Co.

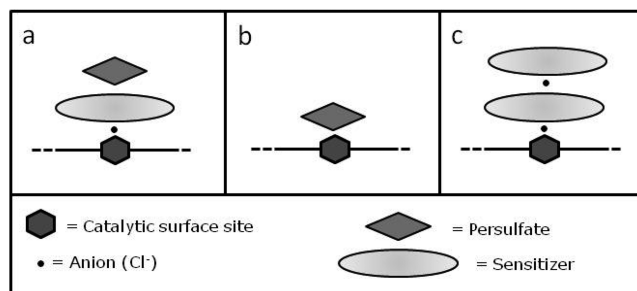
Figure 4 reports the oxygen evolution curves obtained by varying the initial amount of persulfate. As shown in the inset, the initial reaction rate decreases with increasing concentration of persulfate, that is, the apparent reaction order with respect to such reactant is negative. Although dangerous to rely on three points only, the apparent order is not far from –1, and the three points lie on a hyperbola. Chemical yield was also found to decrease with increasing persulfate concentration ( $Y_{(65\text{mg})} = 21.0\%$ ;  $Y_{(260\text{mg})} = 16.3\%$ ;  $Y_{(500\text{mg})} = 4.30\%$ ).

Such a result suggests the involvement of adsorption phenomena in the reaction mechanism. Co cations involved in steps 11 and 12 have to be at the outer surface of the Co-APO-5 particles, if they were accessed by the bulky Ru species, thus acting as adsorption centers for the various species present in solution. Obviously, the main interaction is with negatively charged entities (i.e., *in primis* persulfate, but also HCO<sub>3</sub><sup>–</sup>, SO<sub>4</sub><sup>2–</sup>, and Cl<sup>–</sup> anions). Adsorptive interactions may occur with water molecule themselves and the positively charged Ru species, through the agency of suitable anions (chloride?).

For simplicity, let us consider only persulfate and the Ru complex, accompanied by a Cl<sup>–</sup> anion. Adsorption of the Ru complex and persulfate are depicted in Scheme 2 (structures a and b, respectively). Structure a is the active site, where stripping of an electron occurs readily between the Co center and the Ru complex. Structure b is not active. Adsorption competition between different species may be grossly described by a double Langmuir isotherm:

$$\theta_{\text{Ru}} = K_{\text{Ru}}C_{\text{Ru}}/[1 + K_{\text{Ru}}C_{\text{Ru}} + K_{\text{Per}}C_{\text{Per}}] \quad (13)$$

**Scheme 2. Gross Representation of Three Possible Configurations for the Co Adsorption Centers at the Outer Surface of Co-APO-5 Particles<sup>a</sup>**



<sup>a</sup>(a) Active site (Co center in contact with the Ru complex via a Cl<sup>–</sup> anion); (b) adsorbed persulfate on Co center; (c) less active Co center carrying two Ru complexes with related anions.

where  $\theta_{\text{Ru}}$  is the coverage of Co sites carrying one Ru complex (structure a),  $K_{\text{Ru}}$  is the equilibrium constant for such interaction,  $C_{\text{Ru}}$  is the solution concentration of the Ru complex,  $K_{\text{Per}}$  is the equilibrium constant for the interaction persulfate/Co center (structure b), and finally  $C_{\text{Per}}$  is the concentration in solution of persulfate.

We expect the interaction between persulfate and Co be stronger than that of the Co/Ru complex, which is mediated by another anion. Actually, the amounts of both [Ru(bpy)<sub>3</sub>]<sup>2+</sup> and persulfate overcome that of external Cobalt ions, so that we expect eq 13 to reduce to

$$\theta_{\text{Ru}} \approx K_{\text{Ru}}C_{\text{Ru}}[K_{\text{Per}}C_{\text{Per}}]^{-1} \quad (14)$$

in agreement with what was observed.

This result shows that under the conditions adopted in our case, a large fraction of Ru complex is not effectively used in the WO reaction.

Finally, when persulfate and catalyst amounts are kept constant at 260 and 250 mg, respectively, and [Ru(bpy)<sub>3</sub>]<sup>2+</sup> concentration is changed from 0.60 to 0.27 mM (Figure 5), the slope of the linear portion increases slightly, suggesting also in this case a negative order of reaction with respect to sensitizer, though much less marked than with persulfate. Indeed, when [Ru(bpy)<sub>3</sub>]<sup>2+</sup> concentration is increased to 0.93 mM, the slope

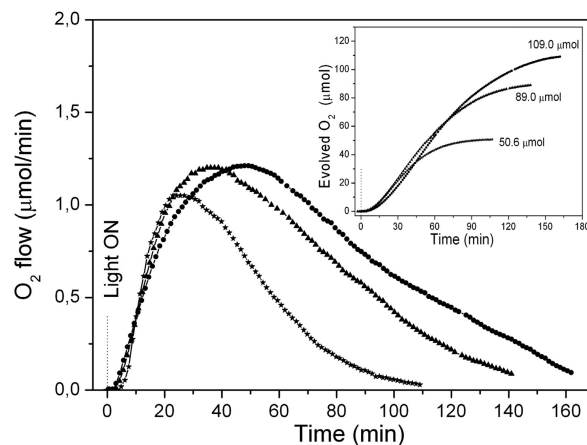


**Figure 5.** Oxygen evolution curves with different amounts of sensitizer: (▲) 45 mg; (★) 20 mg; (●) 70 mg. Inset shows integral amounts of evolved oxygen.

of the linear portion decreases slightly. A very rough estimate of the corresponding reaction order with respect to the sensitizer is  $-0.4$ .

A further indication about the fact that the system performs better at lower sensitizer concentration comes from the comparison of total oxygen evolved and amount of sensitizer (i.e.,  $n(\text{O}_2)/n(\text{Ru}(\text{bpy})_3\text{Cl}_2) = 1.87, 1.48, \text{ and } 1.17$  with sensitizer concentrations of 0.27, 0.60, and 0.93 mM, respectively). We propose as a possible explanation for the partially negative reaction order the formation of sites carrying two Ru complexes, as tentatively depicted in structure c of Scheme 2, where the excitation of one Ru complex is quenched by the other, instead of undergoing the chain of reactions yielding OE.

## CONCLUSIONS

The Co-APO-5 material in the presence of  $[\text{Ru}(\text{bpy})_3]^{2+}$  and persulfate acts as a photocatalyst for WO, in agreement with previous photoelectrochemical results.<sup>23</sup> Decomposition of the sensitizer heavily interferes with the study of the WO process, because it amounts to more than 80% of the total, probably because the electron transfer to  $[\text{Ru}(\text{bpy})_3]^{3+}$  from the catalytic Co center is much slower than the attack by water (or hydroxyls). Sensitizers different from the one adopted and designed "ad hoc" would feature quicker electron transfer.<sup>36</sup>

Some features of the kinetics of WO can be however established, making use of the slope of the initial portion of the oxygen evolution curves as a measure of the initial rate of reaction. The apparent reaction order with respect to the sacrificial reactant is close to  $-1$ , indicating a strong competition with the Ru dye for adsorption on the catalytic center. This is assumed to involve Co ions (maybe a cluster of them) at the outer layer of a Co-APO-5 particle, accessed by the large sensitizer species, at variance with the Co species located in the core of the particle. A limited negative order was also found for the Ru complex, for which a tentative explanation has been advanced.

## ASSOCIATED CONTENT

### Supporting Information

Powder X-ray diffraction, FE-SEM picture of calcined Co-APO-5, and DR UV-vis spectra of Co-APO-5 as-synthesized, calcined, and after contact with  $\text{H}_2\text{O}$ . This material is available free of charge via the Internet at <http://pubs.acs.org>.

## AUTHOR INFORMATION

### Corresponding Author

\*E-mail: [edoardo.garrone@polito.it](mailto:edoardo.garrone@polito.it)

### Notes

The authors declare no competing financial interest.

## ACKNOWLEDGMENTS

Thanks are due to Profs. G. Saracco and P. Spinelli for fruitful discussions, to Dr. S. Esposito for critically reading the manuscript, and to HYSYTECH s.r.l. for reactor development. This research has been carried out in the context of the European Project "SOLHYDROMICS".

## REFERENCES

(1) Yerga, R. M. N.; Galvan, M. C. A.; del Valle, F.; Voilloria de la Mano, J. A.; Fierro, J. L. *ChemSusChem* **2009**, *2*, 471.

(2) Brunshwig, B. S.; Chou, M. H.; Creutz, C.; Ghosh, P.; Sutin, N. *J. Am. Chem. Soc.* **1983**, *105*, 4832.

(3) Ghosh, P. K.; Brunshwig, B. S.; Chou, M.; Creutz, C.; Sutin, N. *J. Am. Chem. Soc.* **1984**, *106*, 4772.

(4) Shafirovich, V.; Khannanov, N. K.; Strelets, V. V. *Nouv. J. Chim.* **1980**, *4*, 8.

(5) Harriman, A.; Pickering, I. J.; Thomas, J. M.; Christensen, P. A. *J. Chem. Soc., Faraday Trans. 1* **1988**, *84*, 2795.

(6) Artero, V.; Chavarot-Kerlidou, M.; Fontecave, M. *Angew. Chem., Int. Ed.* **2011**, *50*, 7238.

(7) Jiao, F.; Frei, H. *Angew. Chem., Int. Ed.* **2009**, *121*, 1873.

(8) Kay, A.; Cesar, I.; Gratzel, M. *J. Am. Chem. Soc.* **2006**, *128*, 15714.

(9) Kanan, M. W.; Nocera, D. G. *Science* **2008**, *321*, 1072.

(10) Reece, S. Y.; Hamel, J. A.; Sung, K.; Jarvi, T. D.; Esswein, A. J.; Pijpers, J. J. H.; Nocera, D. G. *Science* **2011**, *334*, 645.

(11) Zidki, T.; Zhang, L.; Shafirovich, V.; Lymar, S. V. *J. Am. Chem. Soc.* **2012**, *134*, 14275.

(12) Liang, Y.; Li, Y.; Wang, H.; Zhou, J.; Wang, J.; Regier, T.; Dai, H. *Nat. Mater.* **2011**, *10*, 780.

(13) Seabold, J. A.; Choi, K.-S. *Chem. Mater.* **2011**, *23*, 1105.

(14) Pilli, S. K.; Furtak, T. E.; Brown, L. D.; Deutsch, T. G.; Turner, J. A.; Herring, A. M. *Energy Environ. Sci.* **2011**, *4*, 5028.

(15) McCool, N. S.; Robinson, D. M.; Sheats, J. E.; Dismukes, G. C. *J. Am. Chem. Soc.* **2011**, *133*, 11446.

(16) La Ganga, G.; Puntoriero, F.; Campagna, S.; Bazzan, I.; Berardi, S.; Bonchio, M.; Sartorel, A.; Natalic, M.; Scandola, F. *Faraday Discuss.* **2012**, *155*, 177.

(17) Yin, Q.; Tan, J. M.; Besson, C.; Geletii, Y. V.; Musaev, D. G.; Kuznetsov, A. E.; Luo, Z.; Hardcastle, K. I.; Hill, C. L. *Science* **2010**, *328*, 342.

(18) Symes, M. D.; Surendrenath, Y.; Lutterman, D. A.; Nocera, D. G. *J. Am. Chem. Soc.* **2011**, *133*, 5174.

(19) Goberna-Ferrón, S.; Vígara, L.; Soriano-López, J.; Galán-Mascarós, J. R. *Inorg. Chem.* **2012**, *51*, 11707.

(20) Gianotti, E.; Marchese, L.; Martra, G.; Coluccia, S. *Catal. Today* **1999**, *54*, 547.

(21) Saha, S. K.; Waghmode, S. B.; Maekawa, H.; Komura, K.; Kubota, Y.; Sugi, Y.; Oumi, Y.; Sano, T. *Microporous Mesoporous Mater.* **2005**, *81*, 289.

(22) Fan, W.; Fan, B.; Song, M.; Chen, T.; Li, R.; Dou, T.; Tatsumi, T.; Weckhuysen, B. M. *Microporous Mesoporous Mater.* **2006**, *94*, 348.

(23) Garrone, E.; Bonelli, B.; Vankova, S.; Onida, B.; Saracco, G. Italian Patent Request No. TO2011A000895 2011.

(24) Greenwood, N. N.; Earnshaw, A. *Chemistry of the Elements*; Pergamon Press: New York, 1984; p 1295, ISBN 0750633654.

(25) Zanarini, S.; Vankova, S.; Hernandez, S.; Ijeri, V. S.; Armandi, M.; Garrone, E.; Bonelli, B.; Onida, B.; Spinelli, P. *Chem. Commun.* **2012**, *48*, 5754.

(26) Wilson, S. T.; Flanigen, E. M. U.S. Patent 4,567,029, 1986.

(27) Henbest, K.; Douglas, P.; Garley, M. S.; Mills, A. *J. Photochem. Photobiol. A* **1994**, *80*, 299.

(28) White, S. H.; Becker, W. G.; Bard, A. J. *J. Phys. Chem.* **1984**, *88*, 1840.

(29) Hara, M.; Waraksa, C. C.; Lean, J. T.; Lewis, B. A.; Mallouk, T. E. *J. Phys. Chem. A* **2000**, *104*, 5275.

(30) Harriman, A.; Richoux, M.; Christensen, P. A.; Mosseri, S.; Neta, P. *J. Chem. Soc., Faraday Trans. 1* **1987**, *83*, 3001.

(31) Barrett, P. A.; Sankar, G.; Catlow, C. R. A.; Thomas, J. M. *J. Phys. Chem.* **1996**, *100*, 8977.

(32) Montes, C.; Davis, M. E.; Murray, B.; Narayana, M. *J. Phys. Chem.* **1990**, *94*, 6425.

(33) van Breukelen, H. F. W. J.; Kraaijeveld, G. J. C.; van de Ven, L. J. M.; de Haan, J. W.; van Hooff, J. H. C. *Microporous Mater.* **1997**, *12*, 313.

(34) Surendranath, Y.; Kanan, M. W.; Nocera, D. G. *J. Am. Chem. Soc.* **2010**, *132*, 16501.

(35) Hoertz, P. G.; Kim, Y.; Youngblood, W. J.; Mallouk, T. E. *J. Phys. Chem. B* **2007**, *111*, 6845.

(36) Puntoriero, F.; La Ganga, G.; Sartorel, A.; Carraro, M.; Scorrano, G.; Bonchio, M.; Campagna, S. *Chem. Commun.* **2010**, *46*, 4725.